Supplemental Inventory

Figure S1

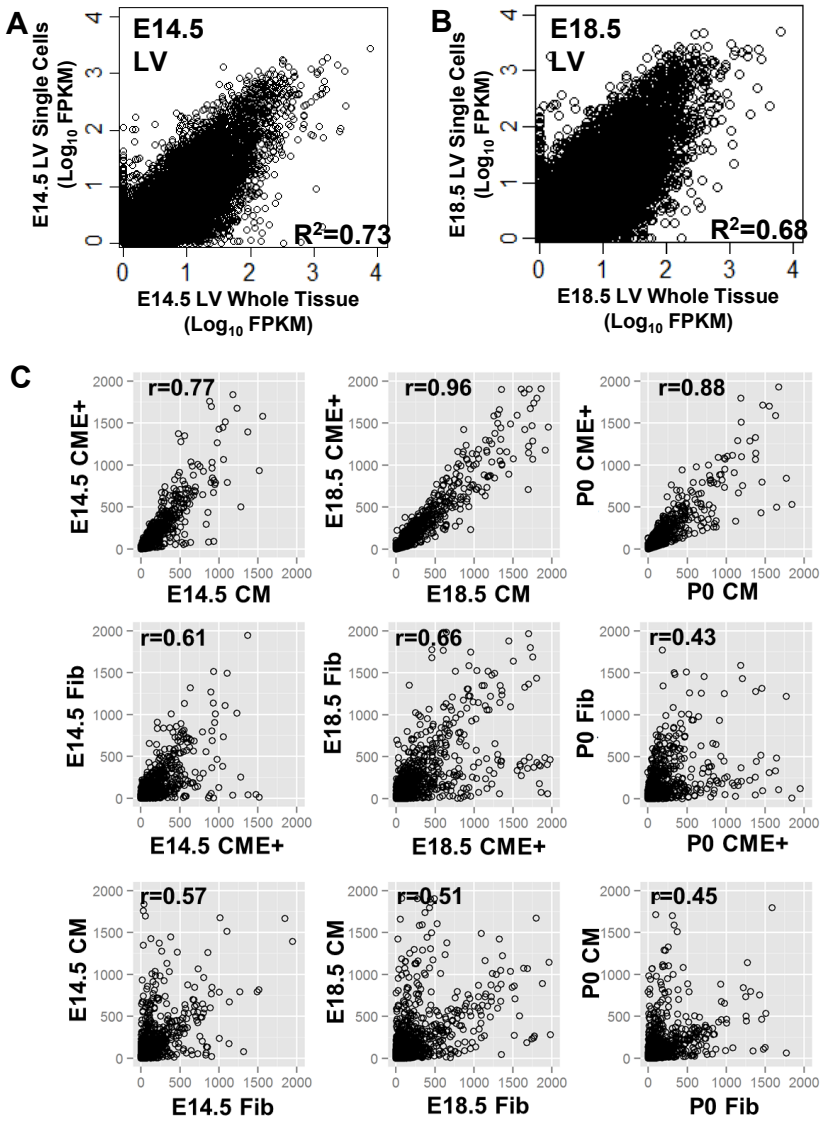
A
E14.5
LV
E14.5 LV Single Cells
(Log10 FPKM)
E14.5 LV Whole Tissue
(Log10 FPKM)
R2=0.73
B
E18.5
LV
E18.5 LV Single Cells
(Log10 FPKM)
E18.5 LV Whole Tissue
(Log10 FPKM)
R2=0.68
C
r=0.77
E14.5 CME+
E14.5 CM
r=0.96
E18.5 CME+
E18.5 CM
r=0.88
P0 CME+
P0 CM
r=0.61
E14.5 Fib
E14.5 CME+
r=0.66
E18.5 Fib
E18.5 CME+
r=0.43
P0 Fib
P0 CME+
r=0.57
E14.5 CM
E14.5 Fib
r=0.51
E18.5 CM
E18.5 Fib
r=0.45
P0 CM
P0 Fib

Figure S2

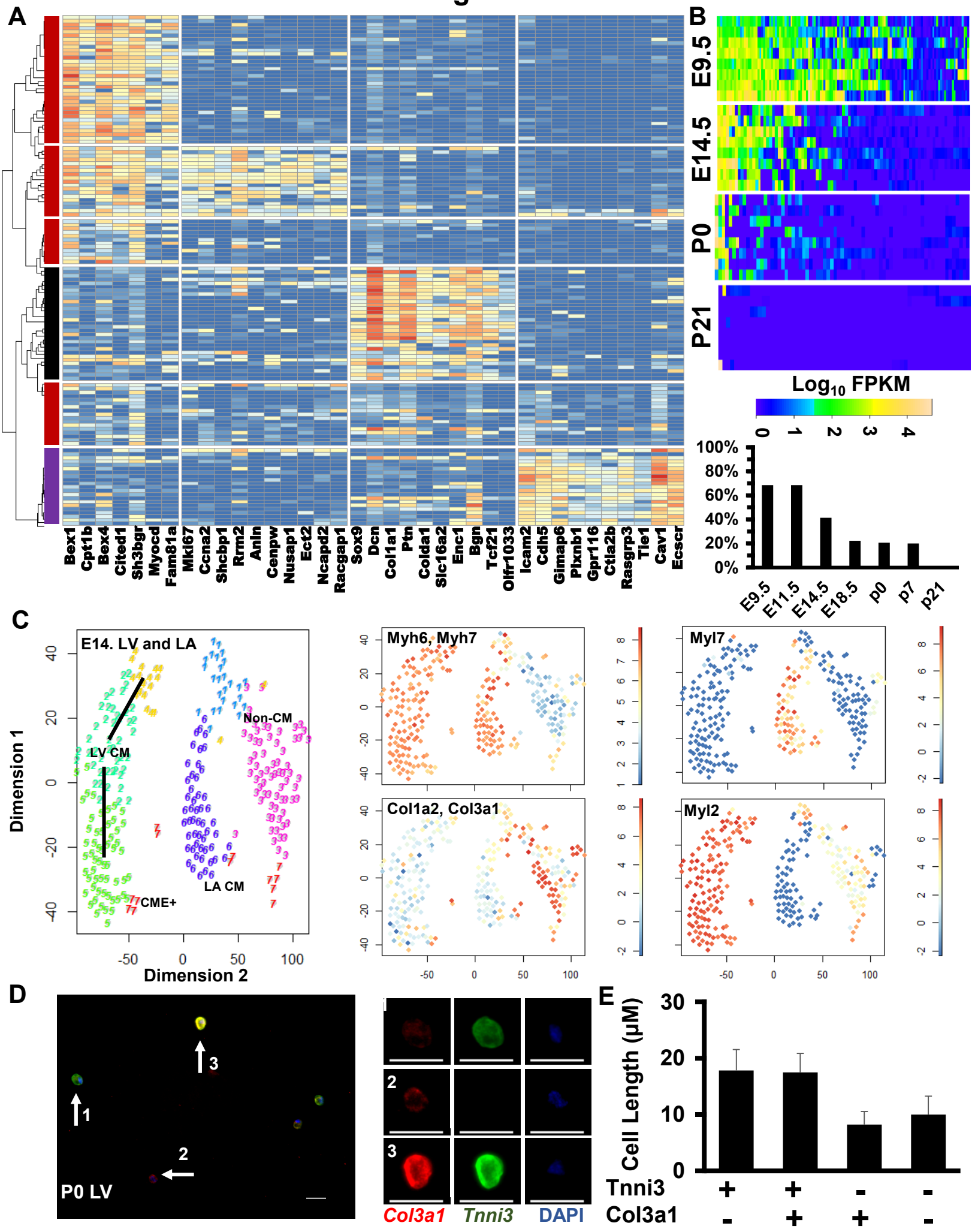
A
Bex1
Cpt1b
Bex4
Cited1
Sh3bgr
Myocd
Fam81a
Mki67
Ccna2
Shcbp1
Rrm2
Anln
Cenpw
Nusap1
Ect2
Ncapd2
Racgap1
Sox9
Dcn
Col1a1
Ptn
Colda1
Slc16a2
Enc1
Bgn
Tcf21
Olfr1033
Icam2
Cdh5
Gimap6
Plxnb1
Gpr116
Ctla2b
Rasgrp3
Tie1
Cav1
Ecscr
B
E9.5
E14.5
P0
P21
Log10 FPKM
0
1
2
3
4
100%
80%
60%
40%
20%
0%
E9.5
E11.5
E14.5
E18.5
p0
p7
p21
C
E14. LV and LA
Dimension 1
Dimension 2
LV CM
Non-CM
LA CM
CME+
Myh6, Myh7
Myl7
Col1a2, Col3a1
Myl2
D
P0 LV
1
2
3
Col3a1
Tnni3
DAPI
E
Cell Length (μM)
Tnni3
Col3a1

Figure S3

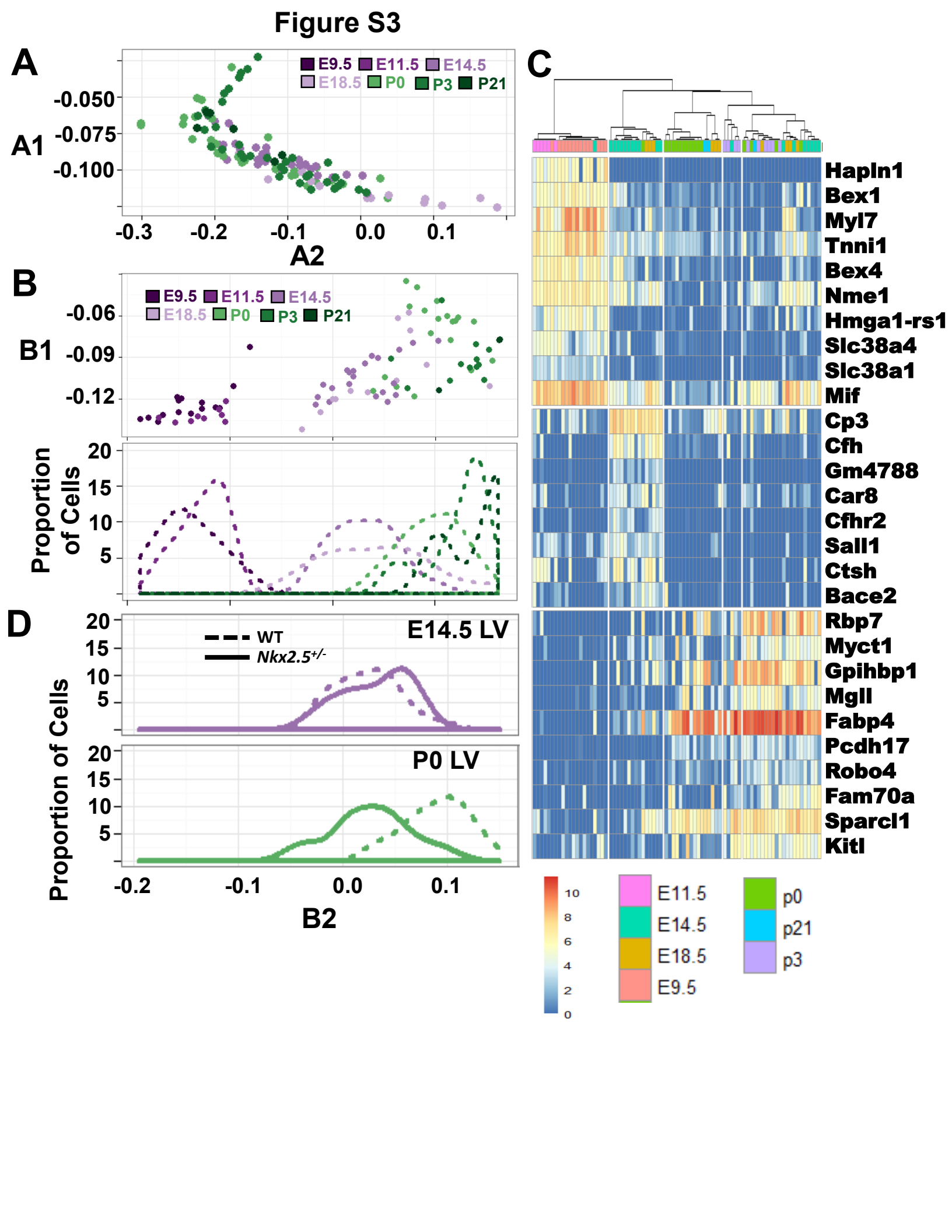
A
E9.5 E11.5 E14.5
E18.5 P0 P3 P21
A1
-0.050
-0.075
-0.100
-0.3 -0.2 -0.1 0.0 0.1
A2
B
E9.5 E11.5 E14.5
E18.5 P0 P3 P21
B1
-0.06
-0.09
-0.12
Proportion of Cells
20
15
10
5
C
Hapln1
Bex1
Myl7
Tnni1
Bex4
Nme1
Hmga1-rs1
Slc38a4
Slc38a1
Mif
Cp3
Cfh
Gm4788
Car8
Cfhr2
Sall1
Ctsh
Bace2
Rbp7
Myct1
Gpihbp1
Mgll
Fabp4
Pcdh17
Robo4
Fam70a
Sparcl1
Kitl
10
8
6
4
2
0
E11.5
E14.5
E18.5
E9.5
p0
p21
p3
D
WT
Nkx2.5+/-
E14.5 LV
P0 LV
Proportion of Cells
20
15
10
5
-0.2 -0.1 0.0 0.1
B2

Figure S4

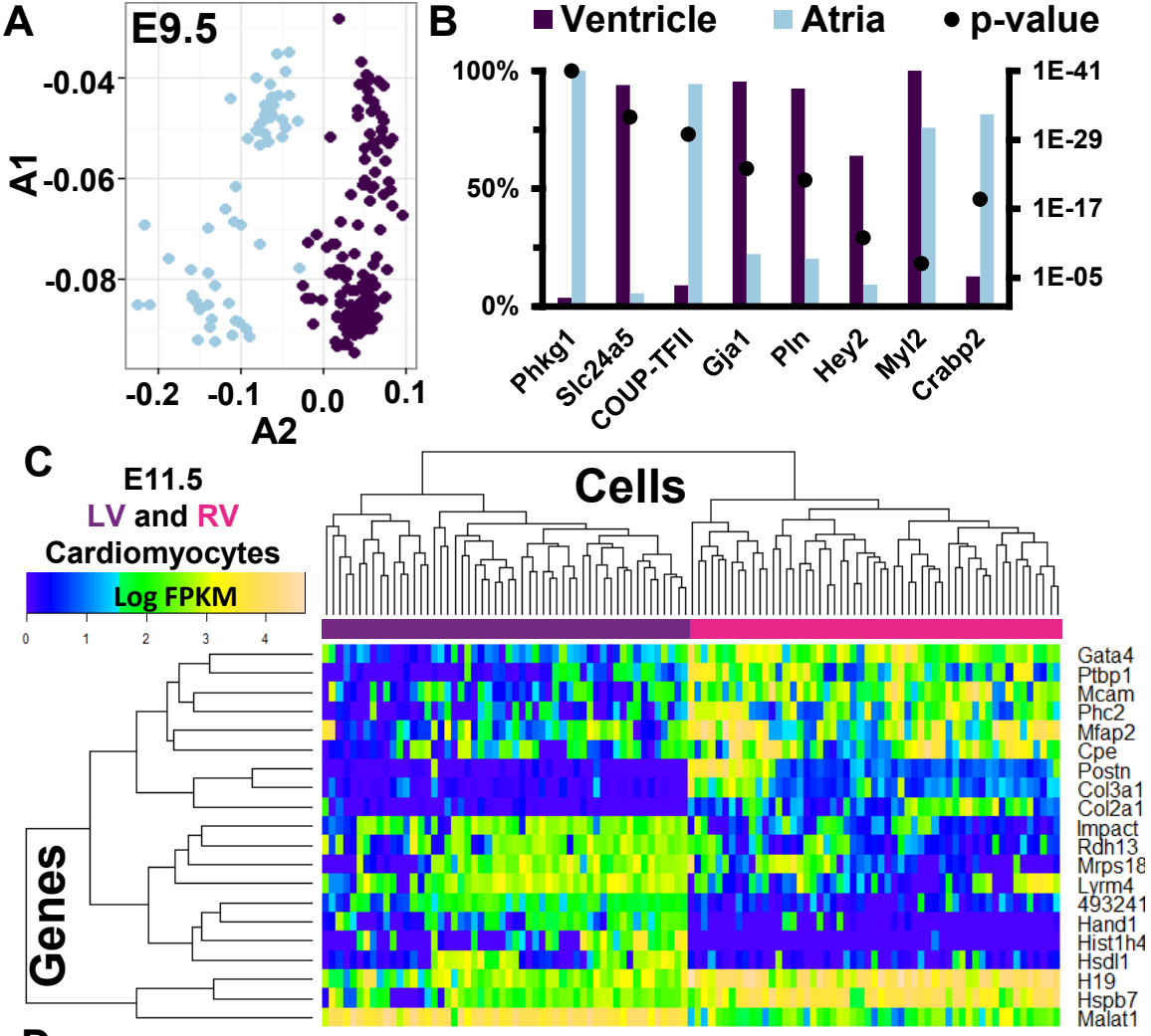

D

Genes Expressed Higher in RV	
Gene Ontology Term	**p-value**
GO:0030198~extracellular matrix organization	2.05E-07
GO:0043062~extracellular structure organization	6.08E-07
GO:0007155~cell adhesion	1.37E-06
GO:0022610~biological adhesion	1.40E-06
GO:0006096~glycolysis	1.94E-06
KEGG Pathway Term	**p-value**
mmu04510:Focal adhesion	1.09E-05
mmu05414:Dilated cardiomyopathy	7.07E-05
mmu05412:Arrhythmogenic right ventricular cardiomyopathy (ARVC)	1.83E-04
mmu04540:Gap junction	3.87E-04
mmu00010:Glycolysis / Gluconeogenesis	9.60E-04

Genes Expressed Higher in LV	
Gene Ontology Term	**p-value**
GO:0006730~one-carbon metabolic process	4.93E-04

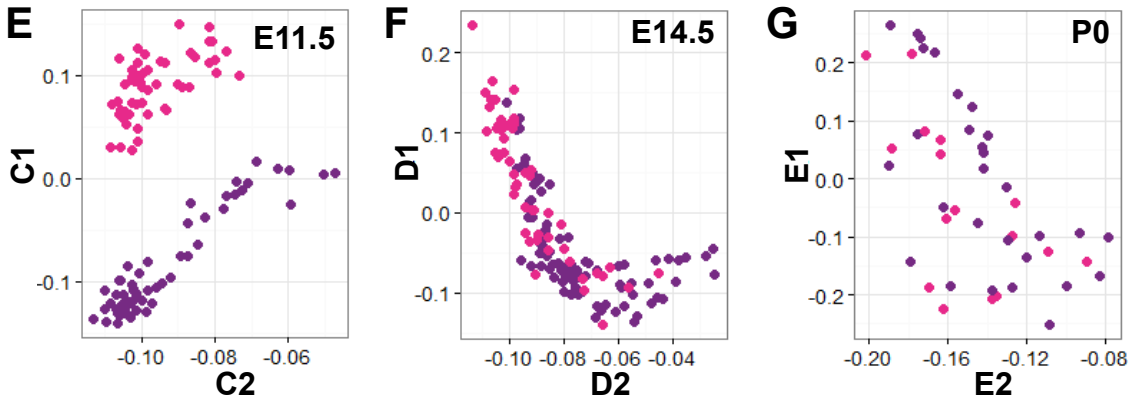

Figure S5

A

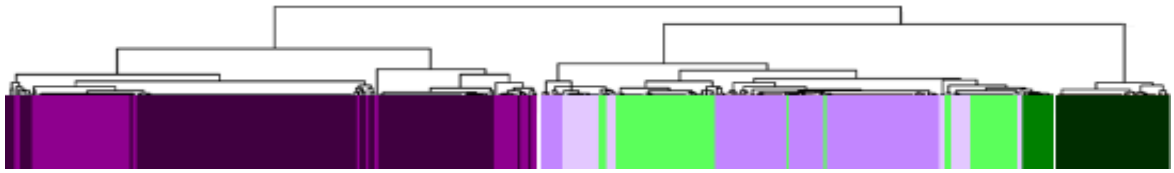

B

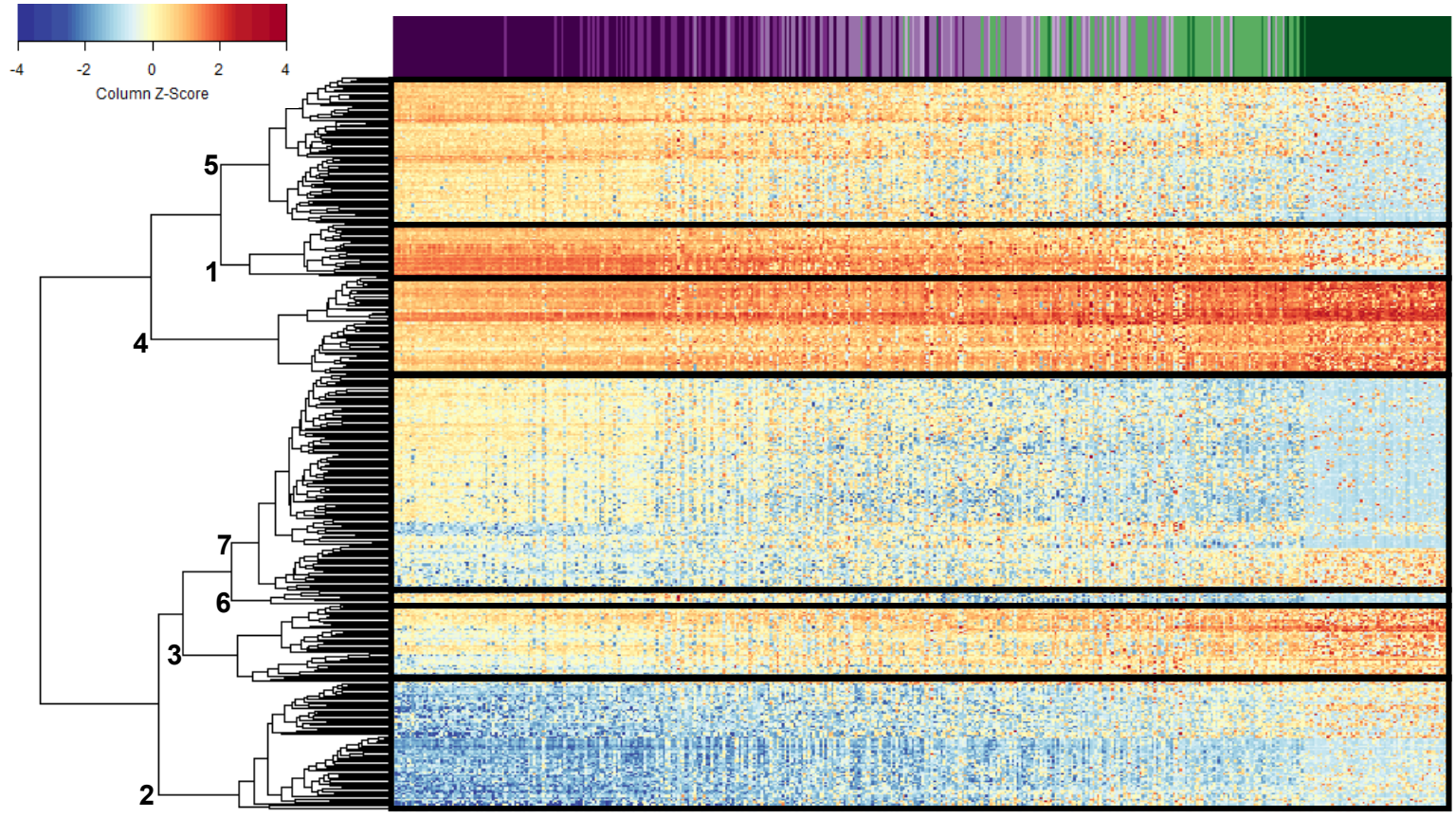

C

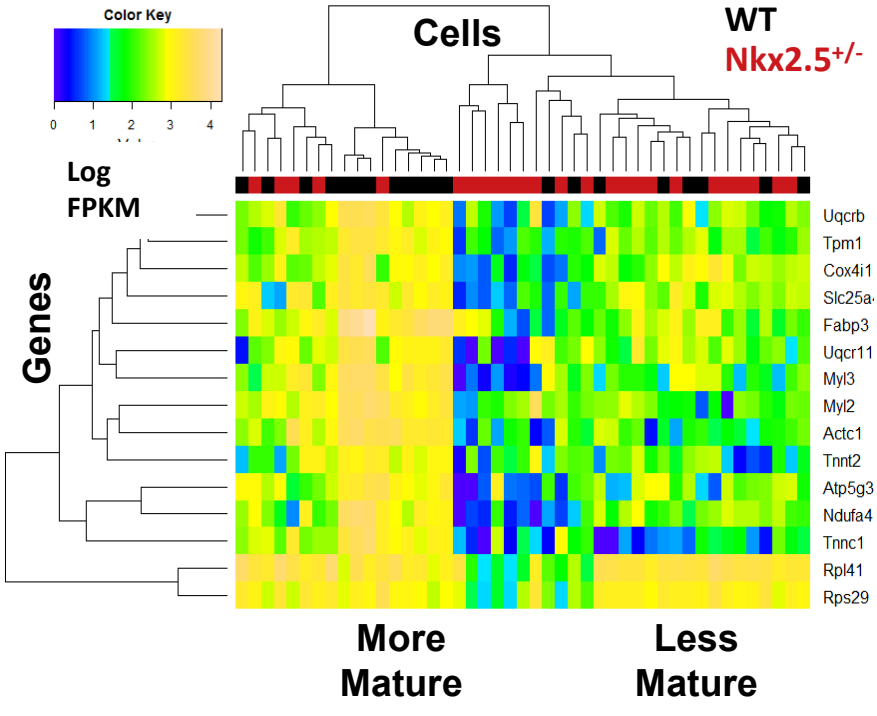

D

***Nkx2.5* Expression at E14.5**

WT	Total Cells	>1 FPKM
Cardiomyocyte	87	32 (36%)
Endothelial	21	1 (4%)
Fibroblast-like	30	0 (0%)
***Nkx2.5*$^{+/-}$**	**Total Cells**	**>1 FPKM**
Cardiomyocyte	32	0 (0%)
Endothelial	10	1 (10%)
Fibroblast-like	20	2 (10%)

***Nkx2.5* Expression at P0**

WT	Total Cells	>1 FPKM
Cardiomyocyte	73	15 (21%)
Endothelial	19	0 (0%)
Fibroblast-like	32	0 (0%)
***Nkx2.5*$^{+/-}$**	**Total Cells**	**>1 FPKM**
Cardiomyocyte	17	5 (29%)
Endothelial	14	1 (7%)
Fibroblast-like	26	0 (0%)

Supplemental Figure Legends

Figure S1, related to Figure 1 and Figure 2: Correlation between RNA-seq data derived from single-cell and whole tissue samples. For each gene, the log of the median FPKM (fragments per kilobase of transcript per million mapped reads) of LV cells isolated at **A)** E14.5 or **B)** E18.5 was plotted against to the log FPKM measured from whole LV-free wall at the same time point. The R^2 comparing median single-cell FPKM to whole tissue FPKM demonstrated correlation at E14.5 (R^2=0.73) and E18.5 (R^2=0.68). **C**) Gene expressions for all CMs, fibroblast-enriched cells, or CME+ were averaged at E14.5, E18.5, or P0. At each time point the mean gene expression for a given cell type (fibroblast-enriched- F; myocyte- CM; CME+) was plotted against the other types and the Pearson correlation calculated (r).

Figure S2, related to Figure 2: Single-cell RNA-seq analysis identifies sources of heterogeneity between and within cardiac cell lineages. **A)** Consensus clustering of E14.5 LV cells using SC3 with k=6 (dendrogram). Putative marker genes for each cluster were calculated using SC3 and a heat map of expression of the most significant genes (x-axis) in each cell (y-axis) is shown. Cell identity as determined by PCA; red=CMs, purple=ECs, black=fibroblast-enriched cells **B**). (top) Heat maps depicting CMs (y-axis) with variable expression of genes (x-axis) associated with proliferation (*Prc1, Ccna2, Cdca8, Cdca3, Top2a, Ccnb2, Mki67, Ccnb1*) at developmental time point indicated. (bottom) The proportion of proliferating CMs decreases during development. At P21, no CMs expressed proliferation genes. **C**) Race ID analyses of cells isolated from E14.5 LV, RV, and LA. Left panel shows t-distributed stochastic neighbor embedding map with cells labeled by cluster obtained via k-means clustering (k=7). Right four panels depict the log

transformed expression in each cell for the genes listed. Note that CME+ cells express *Col1a2*, *Col3a1*, *Myh6*, *Myh7,* and *Myl2,* but not *Myl7* (an atrial CM markers) **D**) Immunohistochemical analyses of p0 LV cells identified CMs expressing *Col3* (CME+). Micrographs of p3 LV cells stained with *Tnni3* (green), *Col3* (red), or Dapi. Cells with different staining patterns were observed in the left images and cells with 3 distinct patterns were enlarged in the right panels. (1) CMs are positive for *Tnni3* but not *Col3*. (2) Non-CMs are positive for *Col3* but not *Tnni3*. (3) CME+ cells are positive for *Tnni3* and for *Col3*. Other cells (not enlarged) were stained for DAPI but neither *Tnni3* or *Col3* likely include ECs. Scale bar - 20μM. **E**) The mean length and standard deviation (error bars) of cells expressing Tnni3 and/or Col3a1 (Panel C; n= 145) was determined along the long axis.

Figure S3, related to Figure 4: Gene expression profiles of developing cardiac ECs and fibroblast-enriched cells. PCA of fibroblast-enriched cells **(A)** and ECs (**B**) during chamber formation (E 9.5), maturation (E11.5, E14.5) late prenatal (E18.5), perinatal (P0, P3) and neonatal life (P21). **A)** Fibroblast-enriched cells showed no discernable temporal pattern of gene expression. The percent of variance explained each principle component is provided in Table S2. **B**). ECs show overlapping stepwise transcriptional changes throughout development. Density plot of EC PCA component B2. The percent of variance explained each principle component is provided in Table S2. **C**) Unsupervised clustering of gene expression in single LV ECs. Consensus clustering performed with the SC3 tool using a k=5 generated the dendrogram. The heatmap depicts the expression the most significantly enriched genes for each cluster. Note that the first two clusters on the left exhibit striking different expression patterns while the right three clusters have

progressive increase in expression of a set of shared markers. **D)** Density plots PCA component B2 from panel B compare wild-type (dotted lines) and *Nkx2.5*$^{+/-}$ (solid lines) ECs. ECs from *Nkx2.5*$^{+/-}$ mice were less mature than WT (black) at P0 but not at E14.5 or P21.

Figure S4, related to Figure 3 and Figure 1: Distinct temporal and chamber gene expression patterns in CMs. **A)** PCA of E9.5 CM gene expression readily distinguishes atrial (light blue) and ventricular (purple) cells. The percent of variance explained each principle component is provided in Table S2. **B)** Selected genes with significantly different expression in E9.5 atria (light blue) and ventricular (purple) CMs. P-values denote Fisher's Exact Test, corrected for multiple testing (5000 genes expressed per cell). **C)** E 11. 5 CMs were clustered using the genes comprising PCA component B1 in **Fig 2B**. LV and RV CMs were clustered separately. Genes differentially expressed between E11.5 LV and RV CMs include previously identified regulators of chamber formation with differential expression between left and right chambers, such as *Hand1*, *Gata4* and *Hspb7*. Genes that differentiated LV from RV fell into 3 patterns: genes expressed specifically in one chamber (*Hand1*, *Hist1h4*, *Postn*), genes expressed in a larger proportion of cells in one chamber (*Gata4, Mcam, Rdh13*), and gene expressed in cells from both chambers but at a higher level in one (*Malat1, H19, Hspb7)*. **D)** Gene ontology and KEGG Pathway enrichment analysis was performed on genes expressed at significantly higher levels in either the LV (n=141) or the RV (n=38) at E11.5 using DAVID. The most significant gene ontology terms and KEGG pathway terms are shown. **E-G)** PCA analysis of LV and RV CMs isolated at E11.5 (C), E14.5 (D), and P0 (E). Note that global expression in LV and RV CMs converges as cardiogenesis progresses and that at

P0, PCA does not distinguish LV and RV CMs. The percent of variance explained each principle component is provided in Table S2.

Figure S5, related to Figure 4 and Figure 6: Maturation defects in *Nkx2.5*$^{+/-}$ CMs. **A)** Unsupervised clustering of wildtype ventricular CMs isolated at (E9.5, E11.5, E14.5, E18.5, P0, P3, P21) identified three broad transcriptional profiles during cardiogenesis, E9.5-11.5, E14.5-18.5, P0-21. Dendrogram generated by consensus clustering using the SC3 tool with k=3. **B**) Hierarchical clustering of the top 400 genes in wildtype cells that explain the most variance in component A2 from **Fig 4B**. Genes (rows) clustered into distinct patterns and their expression normalized per transcriptome to generate a Z-score. Gene constituents within the seven clusters are listed in **Table S8**. Cells (columns) ordered by their value of component A2 from **Fig 4B**) P7 LV *Nkx2.5*$^{+/-}$ CMs express lower levels of genes associated with CM maturity. Hierarchical clustering was performed using component A2 from **Fig 4B** on LV CMs isolated from WT or *Nkx2.5*+/- pups at P0. Cells were clustered into two groups of more or less mature cells. Maturity was estimated using the position of the cells in the PCA performed in **Fig4B,** which ordered CMs across developmental time based on the expression of genes with increased expression in maturing CMs (*Myl2, Myl3, Fabp3, Tpm1, Tnnt2*). The less mature CMs, which contained most of the *Nkx2.5*$^{+/-}$ CMs, expressed lower levels of these genes compared to the more mature CMs. Significantly more (p=0.013) *Nkx2.5*+/- cells clustered with the less mature cells (20/25 cells) compared to WT (8/20 cells). **D**) Proportion of cells that expressed *Nkx2.5* in single cells isolated at p0 from the LV of WT, *Nkx2.5*$^{+/-}$ mice. *Nkx2.5* was expressed principally in myocytes.

Supplemental Tables

Table S1: Size of microfluidic chip used to capture cells at each timepoint in figure 1B

Timepoint	Tissue	Chip Capture Size
E9.5	Atria	5-10uM
	Ventricle	5-10uM, 10-17uM
E11.5	LV	5-10uM, 10-17uM
	RV	10-17uM
E14.5	LV	5-10uM, 10-17uM
	RV	10-17uM
	LA	10-17uM
E18.5	LV	10-17uM
	RV	10-17uM
P0	LV	5-10uM, 10-17uM
	RV	10-17uM
	LA	10-17uM
P3	LV	10-17uM
P21	LV	17-25uM

Table S2: Top 30 genes by weight in informative components from PCA of developing cardiac cell populations in figures 1C, S3B, S4A, 3A, S5C, S5D, S5E, 4A

Table S3: The top ten genes identified by perfect marker gene analysis of clusters of cells in figure 1C

CM	Endothelial	Fibroblast-enriched
Myh6	**Cd93**	**Col1a2**
Ttn	*Gpr116*	**Col3a1**
Myh7	**Pecam1**	**Col1a1**
Tnnt2	*Klhl4*	**Pde1a**
Actc1	**Rasgrp3**	**Col5a1**
Tnnc1	**Emcn**	**Sox9**
Smpx	**Cav2**	**Thbs1**
Tnni3	**Cdh5**	**Dcn**
Nexn	**Ctla2b**	**Postn**
Sh3bgr	**Lgals9**	**Tcf21**

Table S4: Genes differentially expressed between CMs during cardiac chamber formation at E9.5, E11.5 and E14.5 from Figure S4A, Figure S5, and Figure 6

Table S5: Genes differentially expressed between developmental stages in left atria cells depicted in Figure 3A

Table S6: Genes expressed at greater than 1 FPKM in 75% of cardiomyocytes at P0 used to produce Figure 4B, 5A, 5B, 6A

Table S7: Genes comprising different transcriptional programs in developing CMs from Fig 4C, Fig S6B